Thermal reactions of phosphine with Si(100): a combined photoemission and scanning-tunneling-microscopy study

D.-S. Lin*, T.-S. Ku, T.-J. Sheu

Institute of Physics, National Chiao-Tung University, 75 Bo-Ai Street, Hsinchu 300, Taiwan

Abstract

This study investigates the adsorption and thermal decomposition of phosphine (PH_3) on the Si(100)-(2×1) surface. The adsorption species, dissociation reactions, atomic ordering, and surface morphology of the phosphine/Si(100) surface at temperatures between 300 and 1060 K are examined by scanning tunneling microscopy (STM) and high-resolution core-level photoemission spectroscopy employing synchrotron radiation. The P 2p core level spectra clearly indicate that phosphine molecularly adsorbs at room temperature and partially dissociates into PH_2 and H on a time scale of minutes at low (< 0.2 ML) coverages. An exposure of > 15 Langmuirs (L, 1 Langmuir $= 10^{-6}$ Torr s^{-1}) of phosphine on the Si(100)-(2×1) surface at room temperature produces a saturated and disordered surface. The total amount of P on the saturated surface is ca 0.37 ML as calibrated by the P 2p photoemission intensity. Successive annealing of the saturated surface at higher temperatures converts PH_3 into PH_2, converts PH_2 to P–P dimers, and causes the desorption of PH_3. These processes become complete at ~ 700 K, and the resulting surface is a H/Si(100)-(2×1) surface interspersed with one-dimensional P–P islands. Desorption of hydrogen from that surface occurs at ~ 800 K, and is accompanied by partial displacement of P with Si atoms on the substrate. At 850 K, the Si(100) surface, interspersed with 0.22 ML of two-dimensional islands, is a random alloy of nominal 0.5 ML Si–P heterodimers and 0.5 ML Si–Si dimers. © 1999 Published by Elsevier Science B.V. All rights reserved.

Keywords: Chemical vapor deposition; Phosphine; Photoemission; Scanning tunneling microscopy; Silicon

1. Introduction

Most silicon epitaxy uses the chemical vapor deposition (CVD) technique [1]. In silicon CVD processes, phosphine (PH_3) is frequently added to the Si source gas for in situ n-type doping during deposition. Although the apparently simple adsorption and desorption processes which occur during the interaction of phosphine with Si(100) surfaces have received extensive attention, several

fundamental issues regarding the surface species, their bonding configuration, and their thermal stability remain unclear [2–9].
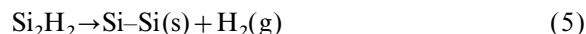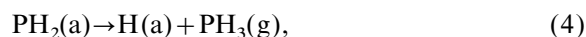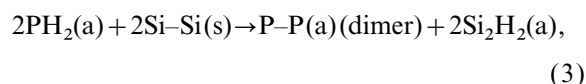
Yu, Vitkavage and Meyerson explored the interaction between phosphine and the Si(100) surface using secondary ion mass spectroscopy (SIMS), Auger electron spectroscopy (AES), X-ray photoelectron spectroscopy (XPS), temperature programmed desorption (TPD) and low-energy electron diffraction (LEED) measurements [2,3]. On the basis of thermal desorption spectroscopy, it was contended that PH_3 adsorption on Si(100)-(2×1) at room temperature is largely molecular

* Corresponding author. Fax: $+886$-3-5729288;
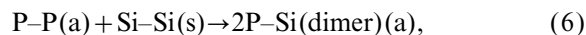e-mail: dslin@cc.nctw.edu.tw.

with a sticking coefficient of near unity and annealing PH_3-saturated surface caused partial dissociation of PH_3 at 475 K and hydrogen desorption at 675 K. Their results further indicated that the maximum phosphorus coverage, close to 1-ML ($1 ML = 6.8 \times 10^{14}$ cm^{-2}) at 823 K and 0.25 ML at 300–673 K, strongly varies with the substrate temperature. By employing STM, Wang et al. observed two varieties of protrusions directly on top of a single Si–Si dimer at the initial stage of PH_3 adsorption on Si(100) at 300 K [4]. Although their STM images revealed vacancies having a depth of a step height (1.36 Å), no features were identified as H atoms adsorbed on Si dimers. Therefore, that investigation correlated the two features with molecularly adsorbed PH_3 and ejected silicon from the substrate during PH_3 adsorption, despite the fact that ejecting a silicon dimer requires a significant amount of activation energy (~ 2.5 eV) [10]. In a related investigation, Wang et al. demonstrated that the Si(100) surface consists of P–P dimers at maxima (one full monolayer) phosphorus coverage, and a nearly random alloy of P–P, Si–Si and Si–P dimers at <1 ML phosphorus coverage [5]. Colaianni et al. carefully examined the PH_3/Si(100) system using high-resolution electron energy loss spectroscopy (HREELS), AES and TPD [6]. Based on the appearance of a Si–H stretching mode, they concluded that most of the phosphine adsorbs dissociatively on the Si(100)-(2×1) surface to produce PH_n ($n = 1, 2$) and H species as low as 100 K, in contrast to the above-mentioned nondissociative adsorption model. According to their TPD data, PH_3 desorption peaks appear at 485 and 635 K, and H_2 at 685 and 770 K. Kipp et al. also performed STM measurements of the PH_3 adsorption on Si(100)-(2×1), similarly observing oblong protrusions centered on Si dimers at room temperature [8]. Notably, their total energy calculations indicated that a PH_3 molecule located above the center of a Si–Si dimer is unstable, thereby leading to their conclusion that the phosphine mainly dissociatively adsorbs into P–P dimers between 300 and 500 K. Hamers et al. recently re-examined the PH_3/Si(100)-(2×1) system using Fourier transform infrared spectroscopy (FTIR) and found that phosphine adsorbs both nondissociatively and dis-

sociatively, depending on the flux and coverage during exposure [7].

In light of the above developments, this study presents STM and synchrotron radiation core-level photoemission spectroscopy data for the thermal reactions of PH_3 on Si(100)-(2×1). Complementary in nature, these two techniques allow us to collect detailed surface chemical information and real-space surface images on an atomic scale. The experimental results indicate that the growth of phosphorus on Si(100) using phosphine involves several reaction steps. The relevant reactions are summarized as follows:

$$PH_3(g) \rightarrow PH_3(a), \tag{1}$$

$$PH_3(a) \rightarrow PH_2(a) + H(a), \tag{2}$$

$$2PH_2(a) + 2Si\text{–}Si(s) \rightarrow P\text{–}P(a)(dimer) + 2Si_2H_2(a), \tag{3}$$

$$PH_2(a) \rightarrow H(a) + PH_3(g), \tag{4}$$

$$Si_2H_2 \rightarrow Si\text{–}Si(s) + H_2(g) \tag{5}$$

and

$$P\text{–}P(a) + Si\text{–}Si(s) \rightarrow 2P\text{–}Si(dimer)(a), \tag{6}$$

where (a), (g) and (s) denote an adsorbed surface species, a desorbed gas molecule and a substrate surface species, respectively. The temperatures at which these equations take place heavily rely on the availability of the surface dangling bonds, similar to that found in another CVD system [11]. In addition, the STM images reveal the formation of one-dimensional P–P dimer chains surrounded by Si monohydride in Eq. (3).

2. Experimental

STM measurements were performed in a stainless steel chamber with a base pressure $<1 \times 10^{-10}$ Torr. A bolt-on commercial UHV–STM system was used. The STM tips were electrochemically etched tungsten wires. All images were obtained in a constant current mode with a tunneling current of ~ 0.3 nA. Slight distortions due to thermal drift were not corrected.

The photoemission experiments were performed

in another μ-metal shielded UHV system utilizing a 1.5-GeV synchrotron radiation source in Hsinchu, Taiwan. Light from the storage ring was dispersed by a 6-m low-energy spherical grating monochromator (LSGM). The photocurrent from a gold mesh positioned in the synchrotron beam path was monitored to relatively measure the incident photon beam flux. The PH_3 adsorption, annealing and phosphorus growth were prepared in situ in UHV conditions. Photoelectrons were collected and analyzed by a 125 mm hemispherical analyzer. The overall energy resolution was < 120 meV.

The Si(100) samples were sliced from boron-doped wafers with an electrical resistivity of ∼10 Ωcm, corresponding to a dopant concentration of ∼1.5×10^{15} cm^{-3}. The wafer's misalignment was ca 0.1° towards ⟨011⟩. Substrate cleaning involved outgassing at ∼900 K for ∼12 h followed by d.c. heating to ∼1450 K for a few seconds. Next, phosphine (Voltaix, ultrahigh purity grade) was introduced into the chamber through a precision leak valve. The dosing pressure, in the 10^{-9}–10^{-8} Torr range, was monitored by an ionization gauge not directly facing the sample. The sample was annealed by passing a current through it and its temperature was measured with an infrared (IR) pyrometer. Each annealing lasted for 60 s.

3. Photoemission results

3.1. Phosphorus growth

Fig. 1a and b display the Si 2p and P 2p core-level spectra, respectively, for the Si(100) surface after exposure to 100 L of phosphine at various substrate temperatures. The photon energies used are 136 eV for Si 2p and 160 eV for P 2p. The bottom spectra of Fig. 1a represent a surface-sensitive Si 2p spectrum for the clean Si(100)-(2 × 1) surface and the least-squares analysis results. Following the standard procedure [12], the spectrum is analyzed in terms of three spin-orbit-split components S, S′ and B of identical Voigt line shape (convolution of a Gaussian and a Lorentzian). The B component corresponds to the bulk emission. The S component accounts for the

small shoulder peak located at ca −0.51 eV relative to the bulk. The S′ component is not visually resolved; however, previous studies have confirmed its presence [12,13]. Other investigators have attributed the S and S′ components to emissions from the surface dimer atoms, each having a dangling bond, and the second-layer atoms, respectively [12]. Nevertheless, other assignments are available for the S and S′ components, accounting for the charge asymmetry between two buckled dimer atoms [13]. However, such an uncertainty does not affect the current discussion since our focus is only on the relative intensity of the S component, which is undoubtedly derived from the dimer layer.

The line shapes of Si 2p core level in Fig. 1a after phosphorus growth can be fitted with two components with varying width: one (labeled B) arising from bulk silicon atoms and another (labeled Sp) from the P–Si interface. The energy positions for the B components of the Si 2p spectra in Fig. 1a thus found are used for the relative binding-energy scale for the corresponding P 2p spectra in Fig. 1b. Using this internal energy reference allows us to eliminate the effect of band bending due to the surface changes. All of the other P 2p core-level spectra presented later use the energy reference found in the same manner. According to Fig. 1b, exposure of phosphine at 660 K results in a relatively sharp P 2p line shape. While containing only a pair of spin-orbit-split peaks, the spectrum presumably corresponds to phosphorus emissions from a single bonding environment. All the remaining of P 2p spectra in Fig. 1b also exhibit one spin-orbit-split component although their line shapes broaden. The normalized integrated intensities of P 2p spectra in Fig. 1b account for the relative abundance of surface phosphorus atoms at various adsorption temperatures, and are plotted in Fig. 2a. As Fig. 2a reveals, the photoemission intensity indicates that maximum P coverage takes place at phosphine adsorption temperature of ∼850 K, which corresponds to previous studies [3]. The intensity of the maximum coverage is nominally 1 ML, as indicated in Refs. [3,5,8]. Correspondingly, the total amount of P coverage on room-temperature phosphine saturated Si(100) surface is 0.37 ML.
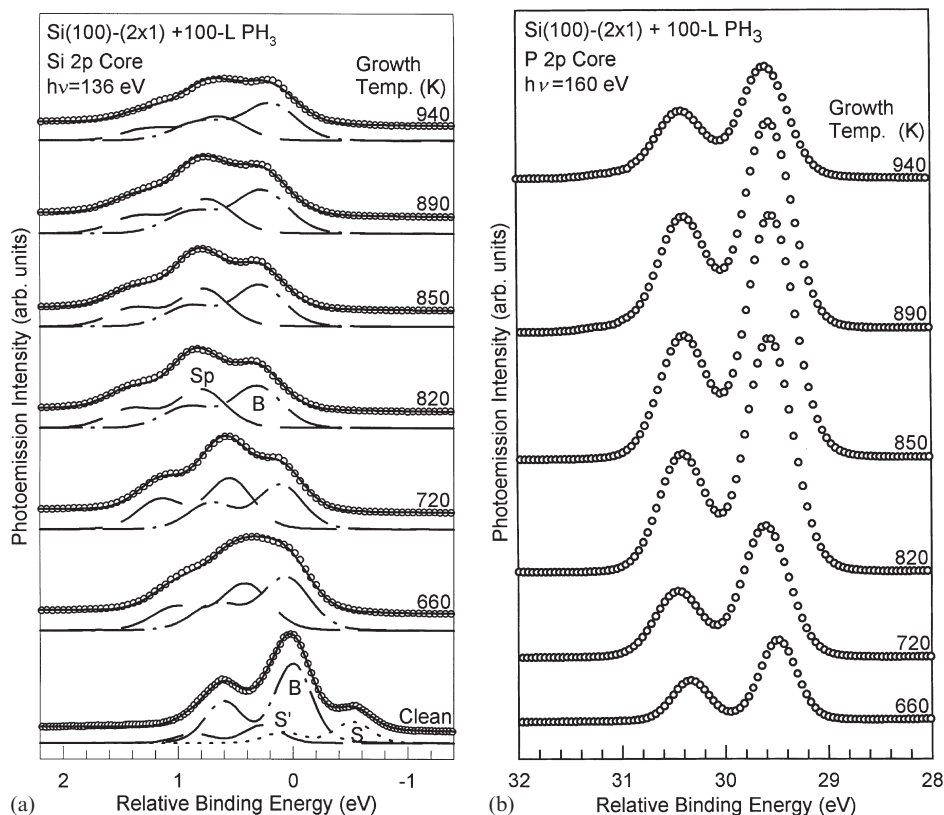
Fig. 1. Photoemission spectra (○) for (a) the Si 2p and (b) the P 2p core levels for phosphine adsorption on Si(100) at various adsorption temperatures as indicated. The solid curves in (a) are fit to the spectra. The curves labeled B, S, S′ and Sp are the results of a decomposition into individual components, each having a pair of spin-orbit-split peaks. The B component is derived from the bulk; S, S′ and Sp are surface related. The relative binding energy of Si 2p core levels refers to the Si $2p_{3/2}$ line of the B component of a clean Si(100)-(2×1). To eliminate the band bending effect, the relative binding energy for P 2p refers to the corresponding Si $2p_{3/2}$ line of the B component. All the Si 2p and P 2p spectra in this paper are presented in this manner.

At growth temperatures between 790 and 890 K, the line shapes of Si 2p core closely resemble each other. The P–Si interface related (Sp) component has a binding energy shift from the B component by 0.49 eV to the higher binding energy side. The normalized total Si 2p intensity after 100-L phosphine adsorption at 850 K decreases by ∼27% from the clean Si(100)-(2×1) surface (bottom spectrum in Fig. 1a). By assuming that a layer (presumably ∼1.4 Å in thickness) of phosphorus attenuates the Si 2p photoelectron signals, an electron escape depth of ∼4.4 Å is derived. This finding correlates well with a typical value of 4 Å for electrons with kinetic energy ≅30 eV [14,15]. Notably, the measured interface-to-bulk intensity

ratio (Sp:B) is 0.92. According to the layer attenuation model, this large ratio implies that 2 ML of silicon atoms underneath the surface phosphorus layer contribute to the Sp component. However, the mechanism for shifting 2 ML S′ core levels to the same energy positions remains unclear.

3.2. Annealing of PH_3 adsorbed Si(100)-(2×1) surfaces

Fig. 3a and b show the Si 2p and P 2p core-level spectra, respectively, for Si(100) surface after exposure to 50-L phosphine at 325 K and followed by successive anneals to higher temperatures. At this dose, the surface is saturated by phosphine
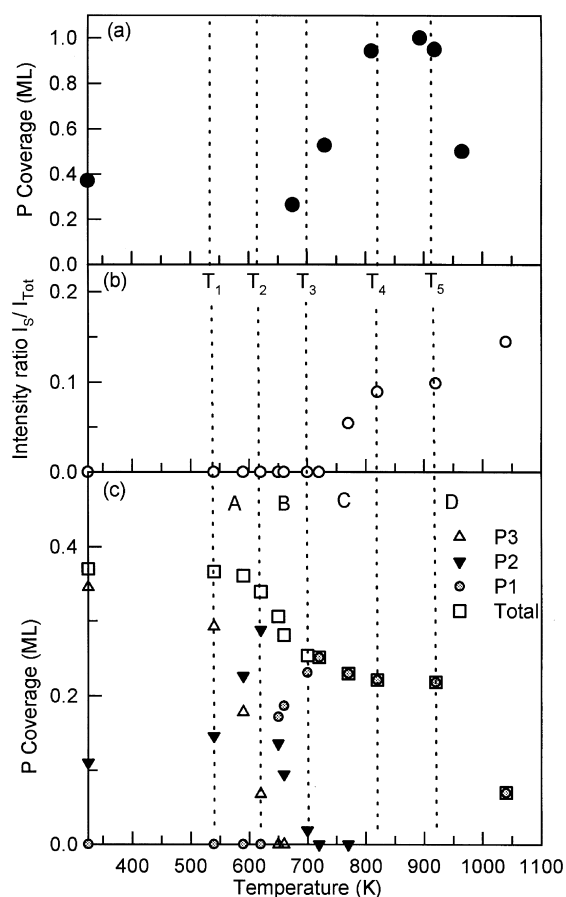
Fig. 2. (a) Phosphorus coverage obtained from FFig. 1b. (b) Intensity ratio of the S component and the total intensity of Si 2p, and (c) photoemission intensity for the P0 ($\bigcirc$, $\bullet$), P2 ($\blacktriangle$), P3 ($\triangle$) components and the sum of the three components ($\square$) of P 2p as a function of annealing temperature. The sample for (b) and (c) is Si(100) initially saturated by a 50 L PH$_3$ exposure at 325 K.

(see Section 3.2) and the S component of the Si 2p spectrum for clean Si(100)-(2 × 1) obviously disappears, indicating that the dangling bonds of the surface dimer layer are passivated. The S component gradually reappears beyond 725 K. Obviously, the line shapes for the Si 2p spectra in Fig. 3a change and shift for increasing annealing temperatures. As mentioned in Section 3.1, the phosphorus-induced component Sp is shifted from the bulk component by +0.49 eV, close to the hydrogen induced chemical shift of ~0.3 eV [16]. To obtain the energy positions for the B compo-

nent of the corresponding Si 2p core, the total integrated intensity (I_{Tot}), and the intensity of the S component (I_S), the Si 2p spectra in Fig. 3a are fitted with three components, S, B and S$_{PH}$, with varying width. The S$_{PH}$ component simulates the mixture of the phosphorus and hydrogen shifted components; its energy position is set at +0.4 eV relative to B. Fig. 2b plots the intensity ratio, I_S/I_{Tot}. After annealing at 1040 K for 60 s, the intensity ratio is 0.15, which is slightly lower than the value of 0.18 for the original clean surface.

The bottom spectrum in Fig. 3b is obtained from the PH$_3$-saturated surface near room temperature. Its line shape displays three distinct peaks and can be analyzed in terms of two spin-orbit-split components, P2 and P3, as indicated. The relative binding energy of the P2 component is lower than that of P3 by 0.54 eV. As the annealing temperature increases to 540 K, the line shape remains largely the same. Above 540 K, the P2 peak grows at the expense of P3. Upon 620 K annealing, the P 2p spectrum largely consists of one component, that is, P2. Above 620 K, the intensity of the P2 component decreases when a new feature appears on the lower binding energy side, ca 0.29 eV relative to the P2 component. Upon 720 K annealing for 1 min, the spectrum consists of just one relatively sharp spin-orbit-split component (labeled P0). Voigt line shapes are then used to fit the spectrum and the resulting line-shape parameters are as follows: spin-orbit splitting, 0.850 eV; p$_{1/2}$/p$_{2/3}$ intensity branching ratio, 0.50; Lorentzian full-width-at-half maximum, 0.075 eV; and Gaussian full-width-at-half-maximum, 0.394 eV. Above 720 K, although the line shapes for the P 2p broaden, their energy positions remain roughly the same. Annealing above 940 K causes the P 2p signals to decrease. Fig. 2c plots the intensity of the P3, P2, P0 components, and the sum of these three components as a function of annealing temperature. Fig. 2 contains four temperature ranges, denoted as A, B, C and D, in which one or more curves show significantly steeper slopes. Such behavior implies certain transitions or reactions. The relevant temperatures define these ranges are the following: $T_1 =$ 540, $T_2 = 620$, $T_3 = 700$, $T_4 = 820$ and $T_5 = 920$ K.
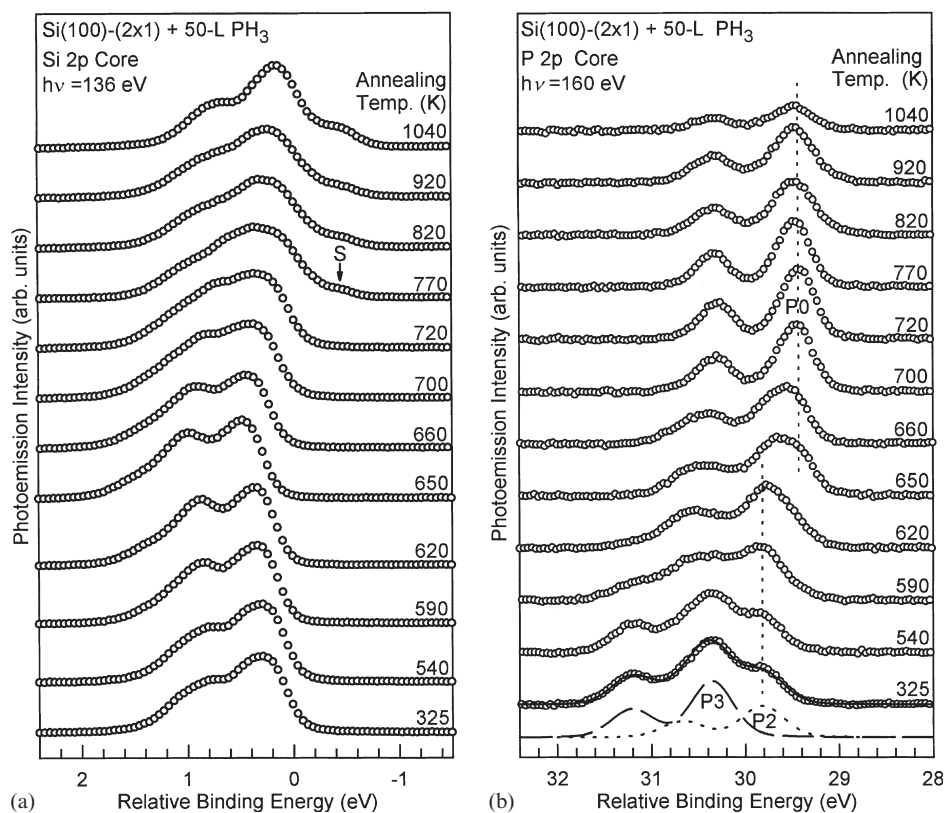
Fig. 3. Photoemission spectra (○) for (a) Si 2p (b) P 2p core levels for various annealing temperatures as indicated. The sample is Si(100)-(2×1) saturated with a 50-L PH$_3$ dose at 325 K. The arrow labeled S in (a) indicates the position for emission from the open dimer atoms (the S component). The fit (solid curve) and the decomposed individual P2 and P3 components for the bottom P 2p spectrum are also shown. The two vertical dash lines in (b) are guides to the eyes for the energy positions of the P2 and P0 components.

3.3. Room temperature adsorption

Fig. 4a and b depict the Si 2p and P 2p core-level spectra, respectively, taken after exposing the Si(100)-(2×1) surface to various exposure levels of phosphine at ~300 K. Upon >2 L of PH$_3$ adsorption, the S component completely disappear and the valley between two spin-orbit-split peaks of the B component fills in. As the phosphine dose accumulates, the integrated photoemission intensity of P 2p spectra in Fig. 4b monotonically increases. In addition, the spectra in Fig. 4b contain three distinct peaks and can be analyzed in terms of two spin-orbit-split components P2 and P3 of identical line shapes. Fig. 5 plots the intensities of the two components and the total intensity

versus the phosphine dose. The total photoemission intensity increases quickly in the initial 2 L exposure and eventually saturates after a total exposure of ~15 L. The intensity is scaled in a manner in which the saturation coverage is set at 0.37 ML based on the measurement shown in Fig. 2a.

4. STM results and discussion

4.1. Room temperature adsorption behavior

As mentioned in Section 1, vibrational bands for PH$_2$ and SiH in HREELS and IR adsorption peaks for PH$_3$, PH$_2$ and SiH are observed upon
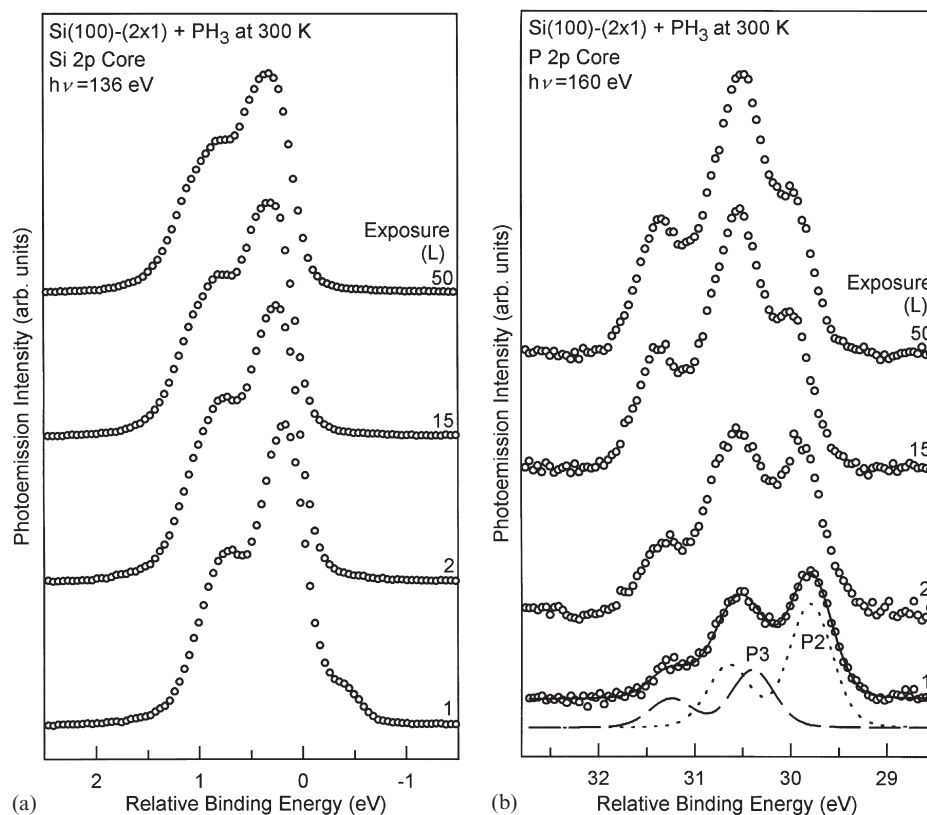
Fig. 4. Photoemission spectra for (a) Si 2p (b) P 2p core levels for various PH_3 exposures on Si(100)-(2×1) at ∼300 K. The fit (solid curve) for the bottom P 2p spectrum is shown, along with the individual P2 and P3 components. The intensity of each spectrum has been normalized to the incident photon beam intensity.

the phosphine adsorption on Si(100)-(2×1) at room temperature, indicating that phosphine dissociatively adsorbs to some extent [6,7]. Owing to that trihydrides generally exhibit a higher chemical shift than dihydrides [16,17], the P3 and P2 components in Fig. 4b can be readily assigned to signals from the adsorbed PH_3 and PH_2 surface species, respectively. Fig. 6 illustrates the overall surface reactions pathways. Both Kipp et al. [8] and Cao et al. [18] calculated the PH_3/Si(100) system, indicating that the PH_3 molecules favor bonding on one end of a Si–Si dimer in the dangling bond positions, as illustrated in configuration A of Fig. 6. The adsorbed PH_3 may decompose to form PH_2 by releasing a hydrogen atom to a nearby Si dangling bond. The dissociated PH_2 radicals may retain its bonding on one end of a Si–Si dimer as proposed in Ref. [7]. In the

STM images such as that in Fig. 7 and those in Refs. [4,8], most adsorption features appear on top of a single dimer. This observation suggests that the dissociation of PH_3 may alternatively take place via insertion of PH_2 into a dimer bond as shown in configuration B of Fig. 6. In this bonding configuration, the phosphorus atom in a PH_2 radical form covalent bonds with two neighboring Si atoms and two H atoms. The fifth valance electron can resonantly form the second valence bond with one of the two neighboring Si atoms and, possibly, prevents the two Si from further PH_3 adsorption. The dissociated H may then attach itself to a nearby Si dangling bond. The overall reaction is energetically favorable since dimer bond breaking requires ∼2.3 eV, while H termination of dangling bonds releases ∼3.6 eV [19]. In configuration B, an adsorbed phosphorus
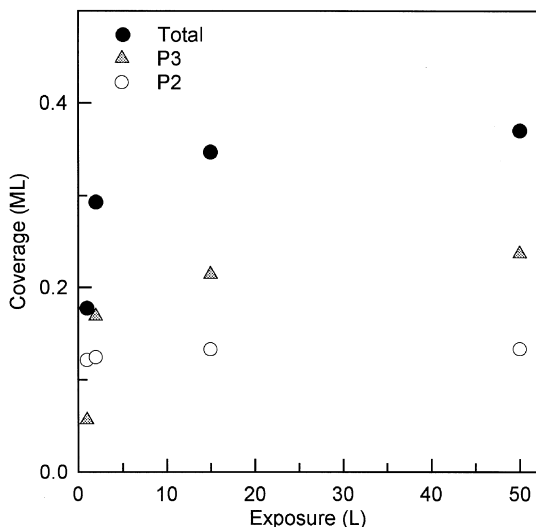
Fig. 5. Coverage of the P2 (○), P3 (▲) components, and the sum of the two components (●) as derived from Fig. 4b. The total coverage for 50-L PH$_3$ exposure is scaled to 0.37 ML (see text).
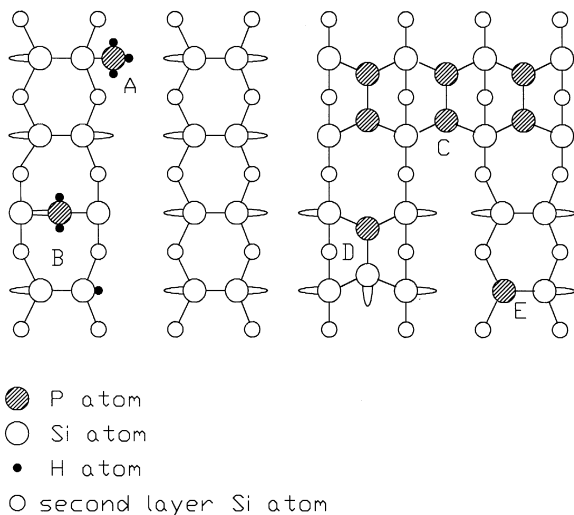

Fig. 7. STM images of the Si(100) surface after exposure to a small amount of PH$_3$ at room temperature. The sample bias used was ~2.3 V.

⬙ P atom
○ Si atom
• H atom
○ second layer Si atom

Fig. 6. Atomic model for the Si(100)-(2×1) surface and schematic diagrams illustrating the various bonding configurations of the PH$_3$ fragments.

atom consumes three free Si sites, thereby leading to the low (~0.37 ML) saturation phosphorus coverage at room temperature.

According to Fig. 5, the intensity of the P3 components with a PH$_3$ dose of <1 L is smaller than that of P2, but continues to increase as
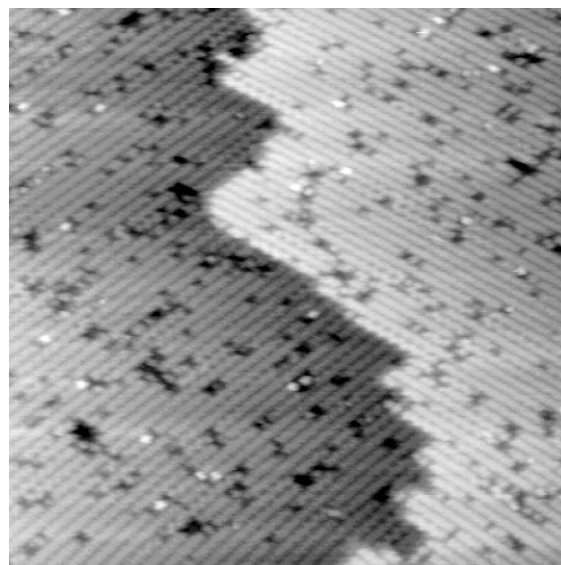
exposure accumulates. In contrast, the intensity of the P2 components remains largely the same for exposure beyond 1 L, implying that the relative abundance of PH$_2$ and PH$_3$ species rely heavily on the total coverage. Upon initial PH$_3$ exposure, a sufficient amount of free surface sites are available, in which the molecularly adsorbed PH$_3$ dissociate into PH$_2$ and H. This dissociation process occurs at a time scale of minutes at room temperature as demonstrated below. Fig. 8 depicts two P 2p spectra taken ~5 and ~30 min after PH$_3$ exposure at room temperature. The intensity ratio of the P2 and P3 components is 1.8 and 3.0 for the lower and the upper spectra in Fig. 8, respectively. Restated, approximately one-third of PH$_3$ molecules dissociate during the ~25-min period (the photon shutter was closed meanwhile). The P 2p line shape beyond 30 min remains largely unchanged, indicating that some PH$_3$ species are stable and probably associated with adsorption around defect sites.

4.2. Transition A

The onset of transition A at T_1 is characterized by a rise of the P2 signal at the expense of P3, as

Si(100)-(2x1) + 0.3-L PH$_3$ at 300 K
P 2p Core
hν=160 eV

min.
30

P3   P2

5

32   31   30   29
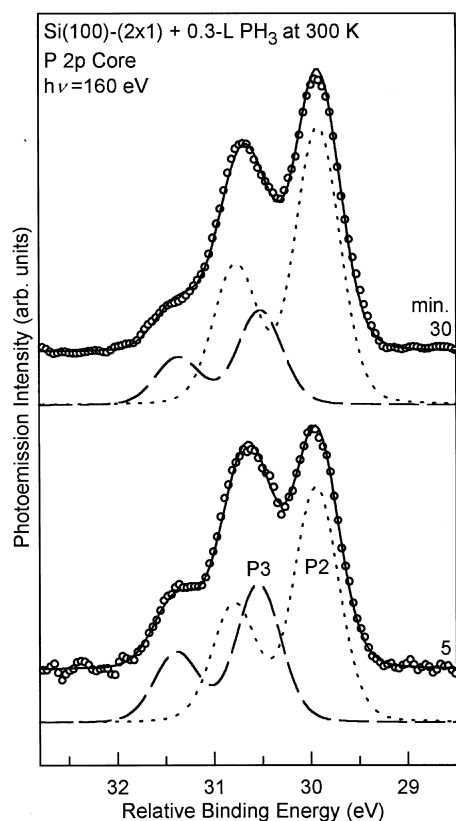Relative Binding Energy (eV)

Fig. 8. Photoemission spectra of P 2p core levels for the Si(100) surface after exposing to 0.3-L of PH$_3$ at 300 K. The lower and upper spectra were taken at about 5 and 30 min after PH$_3$ exposure. The exposure itself lasted ~60 s.

depicted in Fig. 2c. During this transition, the molecularly adsorbed PH$_3$ species gradually dissociates into PH$_2$ and H as indicated by Eq. 2. Fig. 2c also reveals that the total P coverage drops slightly during the transition. This drop is likely attributed to partial desorption of nondissociated PH$_3$ since a previous TPD study reveals a small PH$_3$ desorption peak at 485 K. As mentioned in Section 4.1, the P coverage on room-temperature saturated Si(100) surface is 0.37 ML. However, configuration B in Fig. 6 suggests that dissociated PH$_2$ and H consume three surface sites, resulting in 0.33 ML P coverage at most. The excess adsorbed PH$_3$ of 0.04 ML would have to desorb intact into space, which corresponds to the reduction from 0.37 to 0.34 ML as shown in Fig. 2c. Upon 620 K annealing, the P 2p core in Fig. 3b consists essentially of

a single (P2) component with some broadening possibly due to vibrational excitations as well as a slight amount of the arising P0 component. Halfway through transition A (~580 K), the surface consists of both PH$_2$ and PH$_3$ species and is still highly disordered, as illustrated in Fig. 9a.

4.3. Transition B

Transition B is characterized by a rapid transformation of the P2 component to P0 and a large (~25%) reduction of total surface phosphorus coverage. Fig. 9b and c show the STM images taken after annealing of the room-temperature PH$_3$-saturated surface to the temperatures near the beginning and the end of transition B. Fig. 9b indicates that the adsorption fragments on the surface after 630 K annealing are still disordered, although a chainlike structure is present. Upon further annealing at 730 K, most adsorption fragments line up into short one-dimensional trains, as Fig. 9c depicts. The trains are orthogonal to the dimer rows on the substrate. The substrate dimer rows resemble the (2×1) Si$_2$H$_2$ monohydride structure [20]. Owing to that the desorption maximum of H$_2$ from Si$_2$H$_2$ is ~800 K, the annealing temperature of 730 K is not sufficiently high enough to desorb hydrogen atoms from the surface. Therefore, the substrate dimer rows in Fig. 9c may be readily attributed to Si$_2$H$_2$ dimers. The reduction in P-coverage during transition B correlates with the finding of the molecular phosphine desorption feature at 635 K in TPD spectra [6]. Since both PH$_2$D and PH$_3$ desorption peaks at 635 K are observed on a Si(100) surface partially covered with D species before PH$_3$ exposure, Colaianni et al. contended that phosphine desorption arises from PH$_2$+H recombination as Eq. (4) indicates. Colaianni et al. also observed a H$_2$ desorption peak at 685 K and full removal of the PH$_2$ scissor mode and the P–H stretching mode in HREELS spectra at 650 K, indicating that PH$_2$ (a) undergoes thermal decomposition to P and H near 650 K. The above evidence cumulatively suggests that the dimer-chain features in Fig. 9c are P–P dimers (configuration C in Fig. 6) and contribute to the P0 component in Fig. 3b. All three hydrogen atoms on an adsorbed PH$_3$ molecular
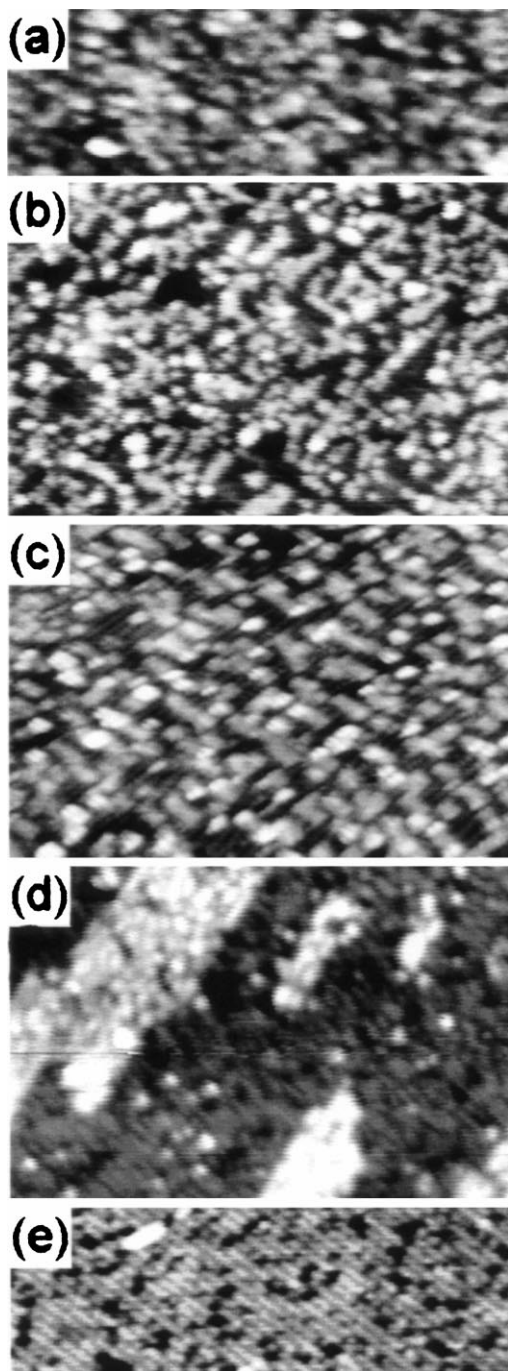
Fig. 9. STM images of the Si(100) surface after annealing to (a) 580, (b) 630, (c) 730, (d) 840 and (d) 1060 K. The sample is Si(100)-(2 × 1) saturated by 20-L PH$_3$ exposure at room temperature. The scanned areas are 100×300 Å^2 for (a, e) and

are released at ~ 700 K. Therefore, as expected, the P coverage is only 0.25 ML, which corresponds to the measured photoemission intensity in Fig. 2c. Again, the excess PH$_2$ fragments desorb from the surface as described in Eq. (4).

4.4. Transition C

During transition C (between 700 and 820 K), the saturation phosphorus coverage surges rapidly from a minimum to a maximum, as depicted in Fig. 2a. Also, according to Fig. 2b, the S component of the Si 2p spectra for the annealed Si(100) surface initially saturated by PH$_3$ at room temperature, recovers half of its intensity. Owing to that the S component in Si 2p spectra characterizes the dimer atoms, its gradual reappearance suggests the hydrogen desorption from Si$_2$H$_2$ monohydrides [Eq. (5)]. The observation of this reaction temperature region fairly corresponds to the β_1 desorption state centered at 780 K for the monohydride Si surface in the TPD spectra. As mentioned in Section 4.3, all hydrogen on adsorbed PH$_3$ molecules are released at ~ 700 K and, along with phosphorus, terminate all surface sites. Therefore, as expected, the P coverage is at the minimum value of only 0.25 ML during phosphine exposure at 700 K, which correlates with the measured photoemission intensity in Fig. 2a. In contrast, all hydrogen desorbs immediately upon PH$_3$ exposure at ~ 800 K, and all surface sites are available for phosphorus, leading to the maximum P coverage of ~ 1 ML.

Annealing the surface such as that of Fig. 9c to 840 K causes the one-dimensional chains to disappear and two-dimensional islands to form, as depicted in Fig. 10a. Notably, the large number of the two-dimensional islands cover $\sim 22\%$ of the surface. Similar to Si molecular-beam epitaxy on Si(100)-(2 × 1) at a substantially lower temperature of ~ 600 K, the two-dimensional islands have typically very anisotropic shapes. In contrast to Fig. 9c, the close-up image (Fig. 9d) reveals no

200×300 Å^2 for (b–d). The sample bias used was $+2.5$ V for (a–d) and -2 V for (e). A monoatomic step can be discerned around the upper right corner in (c).
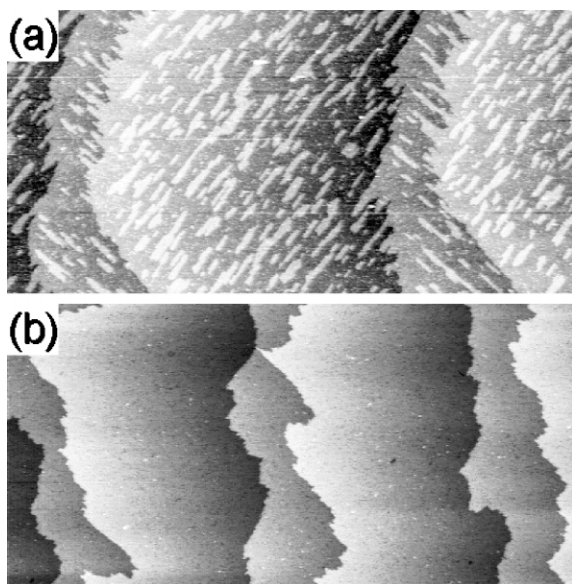
Fig. 10. Large area STM image for the same surface of Fig. 9d and e. The area is 2000×4000 Å^2.

apparent atomic order on both the two-dimensional islands and the substrate, although dimer rows can be discerned on the substrate in some tip conditions (see the lower corner of Fig. 9d). This occurrence clearly subjects that phosphorus atoms randomly disperse on the two-dimensional islands as well as the substrate surface in the energetically more favorable form of Si–P heterodimers (configuration D and E), as Ref. [5] proposes. As described in Section 4.2, P–P dimers, not observed on the H-free Si(100) here, are stable on the Si$_2$H$_2$ monohydride surface. Thus, hydrogen likely hinders phosphorus from displacing silicon on the substrate below ~ 800 K.

An adsorbed phosphorus atom can either incorporate into one of the two-dimensional islands or displace a substrate silicon atom, which diffuses on the surface and eventually incorporates into a two-dimensional island. Consequently, the island coverage of 0.22 ML in Fig. 10a reflects the total coverage of phosphine, even though the two-dimensional islands actually consist not only of P but also of Si. The photoemission measurement of P coverages in Fig. 2c clearly supports this assumption.

4.5. Transition D

Transition D involves the thermal desorption of phosphorus on the surface. Annealing the phosphorus covered Si(100) surface beyond 920 K decreases the P 2p photoemission intensity, as depicted in Fig. 2c. Such a decrease is attributed to the phosphorus desorption in the form of P$_2$, as demonstrated by TPD spectra [9]. STM images (Figs. 9e and 10b) reveal that the Si(100) surface is smooth and the dimer reconstruction is largely restored after annealing at 1060 K for 60 s. In addition, the P$_2$ desorption rate depends mainly on the substrate temperature and surface P coverage. During the continuous PH$_3$ exposure beyond T_5 (920 K), the P coverage reaches saturation when the P adsorption rate equals the desorption rate. The saturation P coverage reaches maximum (1 ML) at temperatures immediately before transition D since the P desorption rate is negligible, but decreases abruptly beyond T_5 as P desorption begins to occur, as depicted in Fig. 2a.

5. Summary

Combining atomic-scale microscopy (STM) and high-resolution spectroscopy (core-level photoemission) techniques provided further insight into the adsorption and thermal reactions of phosphine on the Si(100)-(2×1) surface. This is one of the simplest CVD systems available. Based on the results in this study, we can conclude the following:
1. Phosphine initially molecularly adsorbs on Si(100) at room temperature, but dissociates into PH$_2$ at low coverages on a time scale of minutes. At higher coverages (>0.18 ML), a slight amount of adsorbed PH$_3$ converts to PH$_2$ owing to the lack of nearby surface dangling bonds.
2. The conversion of the remaining adsorbed PH$_3$ into PH$_2$ is a fairly gradual process, again due to the lack of free surface sites. This reaction completes at ~ 620 K.
3. When the PH$_2$ radicals release hydrogen, phosphorus tends to form one-dimensional dimer

chains on the surrounding Si monohydride substrate.

4. The total phosphorus coverage is 0.37 ML on room-temperature PH_3-saturated Si(100) surface, but reduces to nominal 0.25 ML upon annealing to 700 K via the desorption of PH_3. This phenomena is owing to that the surface sites of three times of that amount (0.75 ML) are consumed by dissociated hydrogen.

5. The final surface after annealing a phosphine-saturated Si(100) surface is a random alloy of Si–P and Si–Si dimers; and

6. Equilibrium phosphorus coverage during continuous PH_3 exposure is governed by the surface hydrogen coverage at low temperatures and by the competition between PH_3 adsorption rate and the desorption rate of P_2 at high adsorption temperatures.

Acknowledgements

References

[1] C.W. Pearce, VLSI Technology, McGraw-Hill, New York, 1983, Chap. 2.
[2] M.L. Yu, B.S. Meyerson, J. Vac. Sci. Technol. A 2 (1984) 446.
[3] M.L. Yu, J.J. Vitkavage, B.S. Meyerson, J. Appl. Phys. 59 (1986) 4032.
[4] Y. Wang, M.J. Bronikowski, R.J. Hamers, J. Phys. Chem. 98 (1994) 5966.
[5] Y. Wang, X. Chen, R.J. Hamers, Phys. Rev. B 50 (1994) 4534.
[6] M.L. Colaianni, P.J. Chen, J.T. Yates, J. Vac. Sci. Technol. A 12 (1994) 2995.
[7] J. Shan, Y. Wang, R.J. Hamers, J. Phys. Chem. 100 (1996) 4961.
[8] L. Kipp, R.D. Brigans, D.K. Biegelsen, J.E. Northrup, A. Garcia, L.E. Swartz, Phys. Rev. B 52 (1995) 5843.
[9] M.L. Jacobson, M.C. Chiu, J.E. Crowell, Langmuir 14 (1998) 1428.
[10] J. Wang, T.A. Arias, J.D. Joannopoulos, Phys. Rev. B 47 (1993) 10497.
[11] D.-S. Lin, K.-H. Huang, T.-W. Pi, R.-T. Wu, Phys. Rev. B 54 (1996) 16958.
[12] D.-S. Lin, T. Miller, T.-C. Chiang, Phys. Rev. Lett. 67 (1991) 2187.
[13] L. Pattey, E.L. Bullock, T. Abukawa, S. Kono, L.S.O. Johansson, Phys. Rev. Lett. 75 (1995) 2538.
[14] F.J. Himpsel, F.R. McFeely, J.F. Morar, A. Taleb-Ibrahimi, J.A. Yarmoff, Photoemission and Adsorption Spectroscopy of Solids and Interfaces with Synchrotron Radiation, in: G. Scoles (Ed.), Proceedings of the International School of Physics "Enrico Fermi", North-Holland, New York, 1991, Course CVIII.
[15] T.-C. Chiang, CRC Crit. Rev. Solid State Mater. Sci 14 (1988) 269.
[16] D.-S. Lin, T. Miller, T.-C. Chiang, R. Tsu, J.E. Greene, Phys. Rev. B 48 (1993) 11846.
[17] D.-S. Lin, T. Miller, T.-C. Chiang, Phys. Rev. B 47 (1993) 6543.
[18] P.L. Cao, L.Q. Lee, J.J. Dai, R.H. Chou, J. Phys.: Condens. Matter 6 (1994) 6103.
[19] D. Lubben, R. Tsu, T.R. Bramblett, J.E. Greene, J. Vac. Sci. Technol. A 9 (1991) 3003.
[20] J.J. Boland, Phys. Rev. Lett. 67 (1991) 1539.